A Tomato Vacuolar Invertase Inhibitor Mediates Sucrose Metabolism and Influences Fruit Ripening[1]

Guozheng Qin[2], Zhu Zhu[2], Weihao Wang, Jianghua Cai, Yong Chen, Li Li, and Shiping Tian*

Key Laboratory of Plant Resources, Institute of Botany, Chinese Academy of Sciences, Xiangshan, Haidian District, Beijing 100093, China (G.Q., Z.Z., W.W., J.C., Y.C., S.T.); University of Chinese Academy of Sciences, Yuquanlu, Beijing 100049, China (W.W., J.C., Y.C., S.T.); and Robert W. Holley Center for Agriculture and Health, Agricultural Research Service, United States Department of Agriculture, Ithaca, New York 14853 (L.L.)

ORCID IDs: 0000-0003-3046-1177 (G.Q.); 0000-0002-4352-4061 (L.L.).

Fruit ripening is a complex process that involves a series of physiological and biochemical changes that ultimately influence fruit quality traits, such as color and flavor. Sugar metabolism is an important factor in ripening, and there is evidence that it influences various aspects of ripening, although the associated mechanism is not well understood. In this study, we identified and analyzed the expression of 36 genes involved in Suc metabolism in ripening tomato (*Solanum lycopersicum*) fruit. Chromatin immunoprecipitation and gel mobility shift assays indicated that *SlVIF*, which encodes a vacuolar invertase inhibitor, and *SlVI*, encoding a vacuolar invertase, are directly regulated by the global fruit ripening regulator RIPENING INHIBITOR (RIN). Moreover, we showed that SlVIF physically interacts with SlVI to control Suc metabolism. Repression of *SlVIF* by RNA interference delayed tomato fruit ripening, while overexpression of *SlVIF* accelerated ripening, with concomitant changes in lycopene production and ethylene biosynthesis. An isobaric tags for relative and absolute quantification-based quantitative proteomic analysis further indicated that the abundance of a set of proteins involved in fruit ripening was altered by suppressing *SlVIF* expression, including proteins associated with lycopene generation and ethylene synthesis. These findings provide evidence for the role of Suc in promoting fruit ripening and establish that *SlVIF* contributes to fruit quality and the RIN-mediated ripening regulatory mechanisms, which are of significant agricultural value.

Fleshy fruit ripening is a complex process involving a series of physiological and biochemical changes that influence fruit characteristics such as color, flavor, aroma, and texture (Giovannoni, 2004). Considerable progress has been made in elucidating the biochemical and molecular basis of fruit ripening, including the discovery and characterization of associated transcription factor networks and phytohormone signaling pathways (Alba et al., 2005; Giovannoni, 2007; Klee and Giovannoni, 2011). As an example, the MADS box transcription factor,

RIPENING INHIBITOR (RIN) has been defined as a global regulator of ripening and has been shown to play a key role in modulating ethylene biosynthesis, carbohydrate metabolism, and aroma compound production (Vrebalov et al., 2002; Ito et al., 2008; Qin et al., 2012). Much current research into ripening focuses on the identification of new candidate genes that affect fruit quality traits (Fujisawa et al., 2013; Zhong et al., 2013), an important example of which is flavor.

In general, fruit ripening is characterized by a substantial accumulation of carbohydrates (Fraser et al., 1994) that provide energy for fruit development and contribute to its flavor (Rolland et al., 2002; Zhu et al., 2013), thereby promoting consumption and seed dispersal. Indeed, the content and composition of sugars largely determine fruit sweetness and nutritional quality (Borsani et al., 2009). Although the regulatory effects of sugars on photosynthetic activity and plant metabolism have long been recognized (Godt and Roitsch, 1997; Koch, 2004; Kocal et al., 2008), the role of sugars as signaling molecules in fruit is less understood. In many plant species, the major form of carbohydrate transported from the leaves to the fruit is Suc, which acts as an important form of energy storage/translocation and plays a central role in growth and development. There is also increasing evidence that Suc may play a nonnutritive role as a regulator of cellular metabolism, possibly by altering gene expression (Huber and Huber, 1996; Rolland et al., 2002; Vaughn et al., 2002; Ruan et al., 2010;

Eveland and Jackson, 2012). Suc imported into fruits is degraded into hexoses (Glc and Fru) for various metabolic and biosynthetic processes and resynthesized in the cytosol, vacuole, and apoplast (Koch, 2004). Suc turnover in vivo is catalyzed by Suc synthase (SS) and invertase (Ruan et al., 2010). SS converts Suc into UDP-Glc and Fru in the presence of UDP, whereas invertase hydrolyzes Suc into Glc and Fru in an irreversible reaction (Klann et al., 1996; Ruan et al., 2010).

Invertases play a major role in plant development and in responses to biotic and abiotic stresses and have been suggested to have important regulatory functions in carbon metabolism and development in fruit (Jin et al., 2009). According to their subcellular locations, invertases are classified as cell wall invertase (CWI), vacuolar invertase (VI), and cytoplasmic invertase (CI) or neutral invertase (NI) forms (Sturm, 1999). In tomato fruit, CWI activity is tightly linked with fruit sugar levels (Fridman et al., 2004) and is thought to hydrolyze extracellular Suc when the apoplastic pathway is active (Jin et al., 2009). Since the vacuole is a storage organelle for sugars, VI is believed to modulate the Suc/hexose ratio in fruits. Antisense suppression of *TIV1*, a *VI* gene, in tomato was reported to result in reduced hexose accumulation during fruit ripening (Klann et al., 1996). Similar findings were reported in other fruits, such as grape (*Vitis vinifera*) berry (Davies and Robinson, 1996) and muskmelon (*Cucumis melo*; Yu et al., 2008), suggesting that VI controls the sugar composition in broad range of fleshy fruit. Given the critical role of VI in fruit development and ripening, its activity is likely to be tightly regulated in vivo. Studies have shown that the invertase is regulated by a range of signals at the transcriptional level (Long et al., 2002; Proels and Roitsch, 2009) and that invertase activity is controlled posttranslationally by inhibitor proteins (Hothorn et al., 2004).

Invertase inhibitors bind to invertases to form inactive complexes. Vacuolar invertase inhibitors (VIFs) have been isolated from tobacco (*Nicotiana tabacum*), Arabidopsis (*Arabidopsis thaliana*), and potato (*Solanum tuberosum*; Greiner et al., 1998; Link et al., 2004; Brummell et al., 2011). Moreover, ectopic expression of *Nt-inhh*, a tobacco *VIF*, in potato tubers strongly reduced VI activity and blocked hexose accumulation (Greiner et al., 1999), while heterologous expression of recombinant potato *VIF* (*INH2*) suppressed potato VI activity in vitro (Brummell et al., 2011). However, to our knowledge nothing has been reported regarding the action or significance of fruit VIFs, which, if present, may be important for regulating VI activity and hence the sugar composition of fruits.

Previous studies suggested a link between sugars and pigment metabolism in fleshy fruit: In vitro Suc supplementation promotes color changes in citrus (*Citrus unshiu*) fruit epicarp (Iglesias et al., 2001) and in tomato (*Solanum lycopersicum*) fruit pericarp discs (Télef et al., 2006). However, evidence that the internal quality trait (sugar levels) and external quality trait (color) of fruits are linked in vivo is lacking. Moreover, much remains to be learned about how sugars affect

fruit quality traits and regulate ripening remains. In this study, we identified a set of genes involved in Suc synthesis and degradation, including *VI* and *VIF*, in tomato as direct targets of the ripening regulator RIN. Our findings indicate a role for Suc in promoting pigment biosynthesis and fruit ripening in vivo and establish *VIF* as a novel genetic tool for regulating fruit ripening.

RESULTS

Expression Analysis of Genes Involved in Suc Metabolism during Tomato Fruit Ripening

The Suc metabolic pathway is well established; however, the expression profiles of genes involved in this process during fruit ripening have not been well characterized. Suc metabolism includes the degradation and resynthesis of Suc in the cytosol, vacuole, and apoplast. Several gene families are involved in these processes, including those encoding invertase, invertase inhibitor, Suc synthase, hexokinase, fructokinase, and Suc phosphate synthase (Carrari and Fernie, 2006; Fig. 1A). We identified the orthologs of these genes in tomato in the SOL Genomics Network (SGN; http://solgenomics.net/) databases using the reported gene sequence of each gene family from tomato or another Solanaceous species as a query. A total of 36 genes were identified (Supplemental Table S1), of which 20 have previously been reported (Klann et al., 1992; Elliott et al., 1993; Wang et al., 1993; Kanayama et al., 1997; Menu et al., 2001; Fridman and Zamir, 2003; Lunn and MacRae, 2003; German et al., 2004; Kandel-Kfir et al., 2006; Jin et al., 2009; Goren et al., 2011; Li et al., 2012). The 16 unreported genes were named numerically or on the basis of the results of phylogenetic analysis. The expression of these 36 genes during ripening in wild-type tomato or in fruits at an equivalent stage, based on the number of days after anthesis, in the *rin* mutant during fruit ripening was analyzed by real-time quantitative reverse transcription (qRT)-PCR, using gene specific primers (Supplemental Table S2). To understand the temporal expression of these Suc metabolism-related genes in the overall context of fruit ripening, the expression of ripening marker genes (*RIN*, *NOR*, *LePG*, *EXP1*, *ACS2*, *ACO1*, *PSY1*, *PDS*; Supplemental Table S3) was also determined.

Eleven invertase genes were identified in the tomato genome, of which five are predicted to encode CWI proteins (*LIN5–9*); one encodes a VI (*VI*), and five encode CI (*NI1–5*). The expression of these genes had different patterns from each other in the *rin* mutant during ripening (Fig. 1B). Notably, *LIN8*, *LIN9*, *NI2*, and *NI4* showed higher expression levels in *rin*, whereas *VI* expression was significantly lower in the mutant throughout ripening.

The activity of invertase has been shown to be controlled posttranslationally by binding to inhibitor proteins (Hothorn et al., 2004), forming an inactive complex.
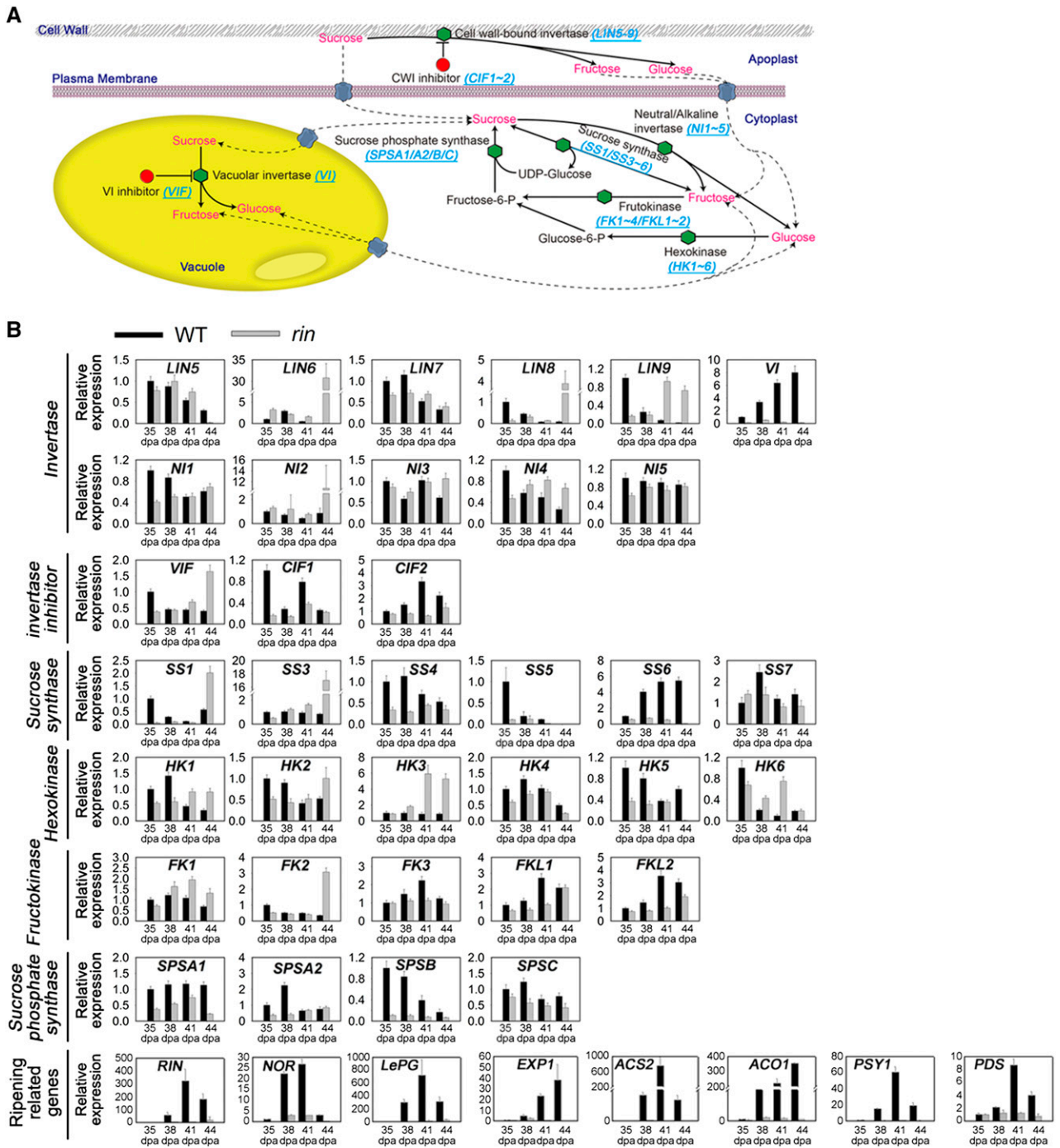
Figure 1. Expression of genes involved in Suc metabolism during fruit ripening. A, Diagram of Suc metabolism in tomato. LIN, Cell wall invertase; VI, vacuolar invertase; NI, cytoplasmic invertase; VIF, vacuolar invertase inhibitor; CIF, cell wall invertase inhibitor; SS, Suc synthase; HK, hexokinase; FK, fructokinase; SPS, Suc phosphate synthase. B, Expression analyses of genes involved in Suc metabolism during fruit ripening in the wild type (WT) and the *rin* mutant by qRT-PCR. The stages of fruit ripening include 35 DPA, 38 DPA, 41 DPA, and 44 DPA. The gene transcript levels are normalized against the *ACTIN* gene, followed by normalization against the wild type at 35 DPA. Values are means ± SD of three independent experiments. The expression of ripening marker genes is shown. RIN, Ripening inhibitor; NOR, nonripening; LePG, polygalacturonase A; EXP1, expansin 1; ACS2, 1-aminocyclopropane-1-carboxylate synthase 2; ACO1, 1-aminocyclopropane-1-carboxylate oxidase; PSY1, phytoene synthase 1; PDS, phytoene desaturase.

Although no inhibitor proteins were identified in the tomato genome for CI, one gene encoding an inhibitory protein, *VIF*, was found for VI, and two inhibitors, *CIF1* and *CIF2*, were identified for CWI. The expression of *VIF* was higher in the fruit of *rin* mutant than in the wild type, while the opposite expression patterns were found

for *CIF1* and *CIF2* (Fig. 1B). These results indicated that RIN promotes the expression of the *VI* gene and suppresses the expression of its inhibitor. Conversely, RIN suppresses the expression of the *CWI* gene and promotes the expression of its inhibitor.

Six Suc synthase genes (*SS1*, *SS3*, *SS4*, *SS5*, *SS6*, and *SS7*) were identified in the tomato genome, which showed different patterns of gene expression from each other in the *rin* mutant at equivalent days after anthesis, and the expression of *SS6* was notably lower in the mutant throughout ripening (Fig. 1B). In addition, six hexokinase genes (*HK1–6*) and six fructokinase genes (*FK1–FKL2*) were identified in the tomato genome. Their expression also showed different patterns from each other in the *rin* mutant during ripening (Fig. 1B), with the exception of the fructokinase gene, *FK4*, whose expression has been specifically linked to stamen development (German et al., 2002) and was not detected in this study. Lastly, four Suc phosphate synthase genes (*SPSA1–SPSC*) were identified, and their expression was shown to be generally lower in *rin* mutant compared with the wild type (Fig. 1B).

ChIP-qPCR Analysis Reveals That RIN Directly Binds to the Promoters of Genes Involved in Suc Metabolism

RIN regulates the expression of ripening-related genes, either directly or indirectly (Fujisawa et al., 2013). To examine whether genes involved in Suc metabolism are also directly regulated by RIN, a chromatin immunoprecipitation (ChIP) assay was carried out. An analysis of the promoter regions of the genes analyzed in this study identified varying numbers of CArG-box binding motifs (Supplemental Table S1), which are elements that are commonly found in MADS-box transcription factor binding sites (Ito et al., 2008). The cross-linked DNA-protein complexes were immunoprecipitated with anti-RIN polyclonal antibody that was prepared using a bacterial expressed recombinant RIN protein. To amplify the promoter sequences surrounding the CArG-box binding sites from the immunoprecipitated DNA, specific primers were designed (Supplemental Table S4), and the binding of RIN to the promoter of *ACC synthase 2* (*ACS2*), a known RIN-target gene (Ito et al., 2008), served as a positive control (Supplemental Fig. S1).

ChIP screening using affinity-purified RIN antibodies, in combination with quantitative PCR (ChIP-qPCR), resulted in an enrichment in the promoter regions of 16 genes compared with when nonspecific antibodies (preimmune rabbit IgG) were used (Fig. 2; Supplemental Fig. S2). Notably, RIN directly bound to the promoter of *VI* and *VIF* (Fig. 2). Taken together with the gene expression analysis showing that *VI* expression was lower in the *rin* mutant than in the wild type, while *VIF* expression was higher (Fig. 1B), these data suggest that RIN modulates Suc degradation in the vacuole during fruit ripening. A similar result was found for genes encoding CWIs, specifically *LIN7* and *LIN8*, and the gene encoding the inhibitory

protein of CWI, *CIF1* (Fig. 2). However, while the expression of *LIN7* and *LIN8* was up-regulated, the expression of *CIF1* was down-regulated in the *rin* mutant during fruit ripening (Fig. 1B). This indicates that Suc degradation associated with CWI is inhibited by the RIN protein during fruit ripening. The ChIP-qPCR analysis also showed that RIN directly bound to the promoter of *NI2* and *NI4* (Fig. 2), which encodes CI. Lastly, RIN was shown to bind directly to the promoter of several other genes involved in Suc metabolism, e.g. *SS3*, *HK3*, and *SPSA1* (Supplemental Fig. S2).

Gel Mobility Shift Assay Confirms That RIN Binds to the Promoters of Suc Metabolic Genes

In order to confirm the binding ability of RIN to the promoter regions of genes identified in the ChIP assay, an electrophoretic mobility shift assay (EMSA) was performed with purified recombinant RIN protein. Specifically we examined the ability of RIN to bind to double-stranded and biotin-labeled probes (Supplemental Table S5) for the genes shown in Figure 2 (*VI*, *VIF*, *LIN7*, *LIN8*, *CIF1*, *NI2*, and *NI4*), which contained CArG-box motifs. For each gene, a band shift was observed when the purified RIN protein was mixed with the biotin-labeled probe (Fig. 3). Formation of the DNA-protein complexes could be prevented by addition of an excessive amount of the corresponding unlabeled probe, indicating specific binding of RIN to the biotin-labeled probe. Based on the different extent of competition by the unlabeled DNA fragment that was observed among these genes, we concluded that RIN had different binding affinities for the promoters of the analyzed genes.

Identification of SlVIF and Assessment of Its Physical Interaction with VI

Having demonstrated that *VI* and *VIF* were directly regulated by RIN, the putative VI inhibitor gene, *VIF*, was chosen for further functional analysis. *VIF* genes have been cloned from Arabidopsis, tobacco, and potato, and reported to modulate Suc metabolism (Link et al., 2004); however, little is known about the expression of *VIF* genes in tomato fruit or their roles in ripening. Tomato *VIF* (GenBank accession no. KC007445; hereafter referred to as *SlVIF*) was cloned based on sequence similarity to the *N. tabacum VIF* (AY145781). SlVIF showed 81% and 71% amino acid identity with NtVIF (Y12806) and StVIF (FJ810206), respectively (Supplemental Fig. S3). All deduced proteins contained the four conserved Cys residues that are a hallmark of all known plant invertase inhibitors (Rausch and Greiner, 2004). We observed that *SlVIF* was expressed in both vegetative and reproductive organs, but at different levels (Fig. 4A). Notably, *SlVIF* mRNA levels were high in fruit, and SlVIF protein
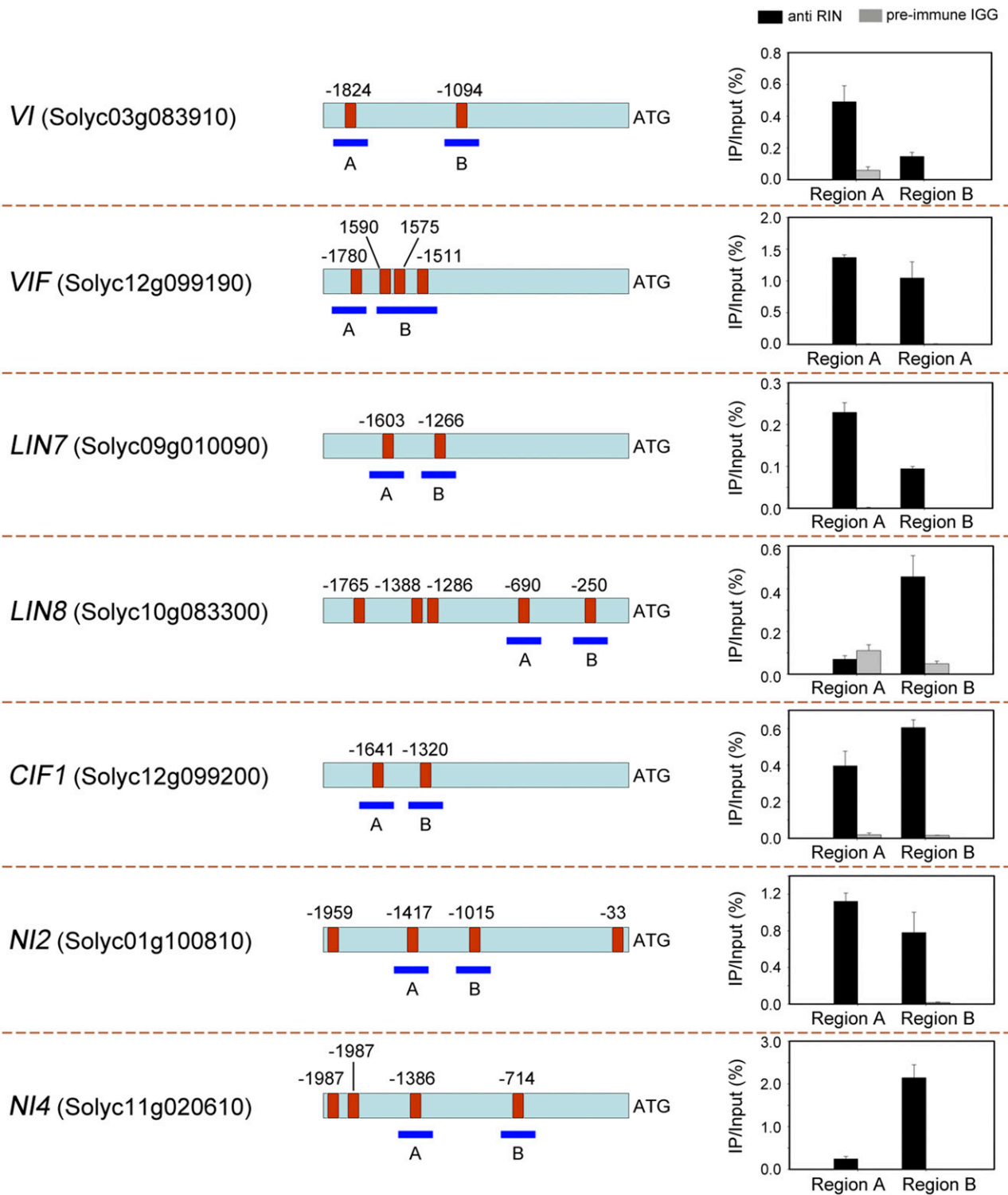
Figure 2. Chromatin immunoprecipition reveals direct binding of RIN to the promoters of genes involved in Suc metabolism. The promoter regions of the target genes are indicated. Red boxes represent CArG-box elements, and numbers above the box indicate the position of these motifs relative to the translational start site. The blue fragments with uppercase letters represent the regions used for ChIP-qPCR. Values are the percentage of DNA fragments that were coimmunoprecipitated with specific anti-RIN antibodies or nonspecific antibodies (preimmune rabbit IgG) relative to the input DNA. Error bars represent the sd of three independent experiments. VI, Vacuolar invertase; VIF, vacuolar invertase inhibitor; LIN, cell wall invertase; CIF, cell wall invertase inhibitor; NI, cytoplasmic invertase.
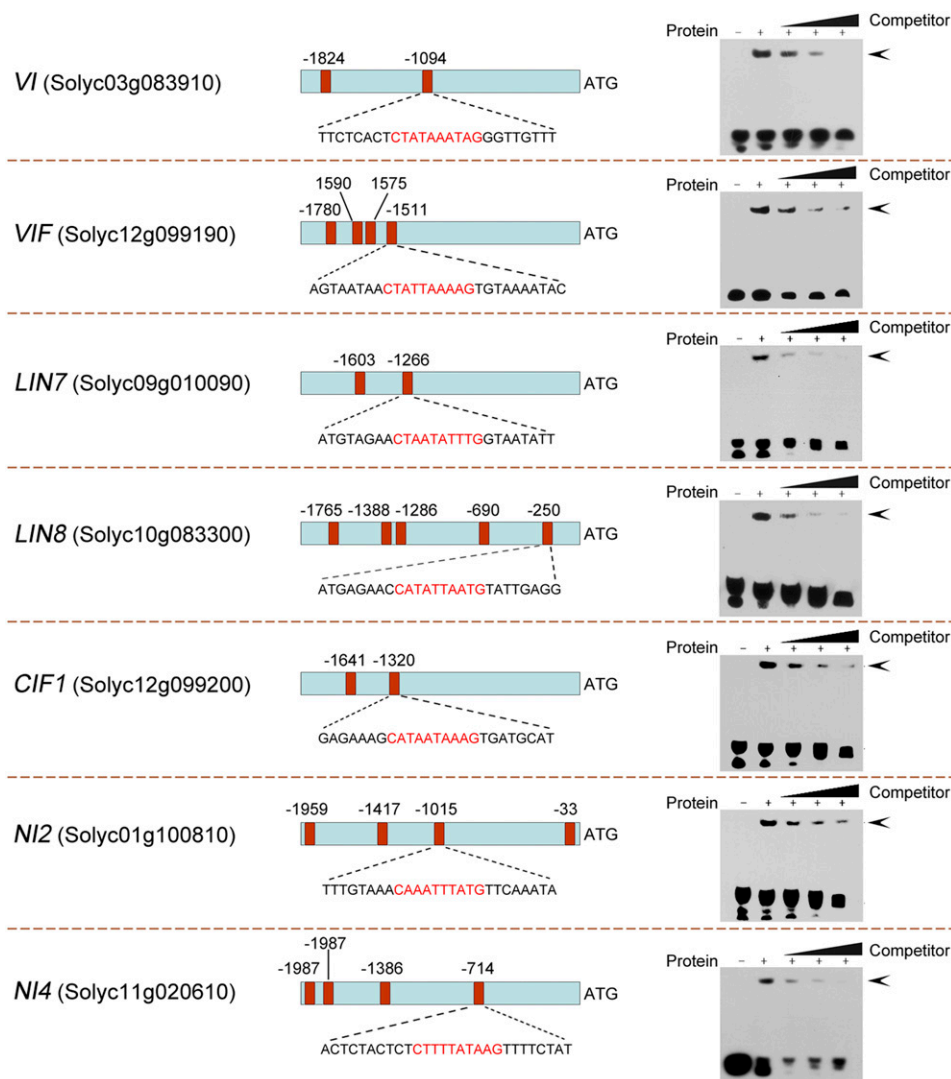
Figure 3. RIN binding to the regulatory regions of target genes revealed by EMSA. The promoter regions of the target genes are indicated. Red boxes indicate CArG-box elements in the promoter region, and numbers above represent the position of these motifs relative to the translational start site. The probe sequences used for EMSA for each target gene are shown, with red letters representing the CArG box. The protein-DNA complexes were separated on 6% native polyacrylamide gels. Triangles indicate the increasing amounts (10×, 100×, or 1000×) of unlabeled probes used for competition. The specific complexes formed are indicated by arrowheads. VI, Vacuolar invertase; VIF, vacuolar invertase inhibitor; LIN, cell wall invertase; CIF, cell wall invertase inhibitor; NI, cytoplasmic invertase.

levels peaked at 38 d post anthesis (DPA) before dropping (Fig. 4B), consistent with *SlVIF* transcript abundance.

To confirm that SlVIF indeed localizes in the vacuole, we transformed tomato with a construct encoding SlVIF fused to a GFP marker, GFP:SlVIF, as well as with a *GFP*-only construct. When we imaged transgenic tomato root cells, we observed that the GFP:SlVIF fusion protein produced a strong signal in the vacuole (Fig. 4C), while the GFP-only control displayed fluorescence throughout the cell (Fig. 4C).

Recombinant SlVIF protein was purified and tested for its inhibitory activity against VI extracted from 44 DPA tomato fruit to confirm whether SlVIF indeed acts as a SlVI inhibitor. As shown in Figure 5A, a decrease in the VI activity was observed upon increasing the SlVIF concentration, while SlVIF had no inhibitory effects on CWI activity. To investigate whether SlVIF physically interacted with SlVI, a yeast two-hybrid (Y2H) assay was performed. The cDNA fragments of *SlVIF* and *SlVI* were cloned into pGBKT7 (BD) and pGADT7 (AD) vectors,

respectively. The resulted plasmids, BD-SlVIF and AD-SlVI, were cotransformed into yeast strains. Yeasts cotransformed with BD and AD, BD-SlVIF and AD, and AD-SlVI and BD were used as controls. As shown in Figure 5B, yeast cotransformed with BD-SlVIF and AD-SlVI displayed normal growth and blue color on the selective SD/-Leu/-Trp/-His/-Ade medium containing X-α-Gal, whereas the controls showed no growth. Taken together, these results indicate that SlVIF interacts with SlVI to suppress SlVI activity.

SlVIF Influences Suc Metabolism and Fruit Ripening

To examine the effects of *SlVIF* on sugar metabolism and fruit ripening, a 35S:*SlVIF* overexpression construct and a *SlVIF* RNAi construct were separately introduced into tomato. Three independent transgenic lines corresponding to each construct and containing single-copy transgenes were identified by qRT-PCR analyses (Mason et al., 2002). The *SlVIF* overexpression line 2 (OE2) and

Figure 4. Characterization of tomato SlVIF. A, qRT-PCR analyses of *SlVIF* in vegetative and reproductive tomato organs. The *ACTIN* gene was used as an internal control. Values are the means of three biological replicates. Bars represent standard deviations. B, Western-blot analysis of SlVIF protein abundance during fruit ripening. Proteins were isolated from fruit at 35 DPA, 38 DPA, 41 DPA, and 44 DPA. An anti-glyceraldehyde-3-phosphate dehydrogenase immunoblot was used as a protein control. In addition, Coomassie Brilliant Blue staining was used as a loading control. C, Subcellular localization of GFP:SlVIF fusion protein. I, to III, Stable expression of the GFP:SlVIF fusion protein in tomato root cells, showing fluorescent signal in the vacuole. IV to VI, Stable expression of GFP alone in tomato root cells, showing fluorescent signals throughout the cell. I and IV show fluorescent images; II and V are the same images viewed using bright-field microscopy. III and VI are overlays of fluorescent and bright-field images. Bar = 10 μm.
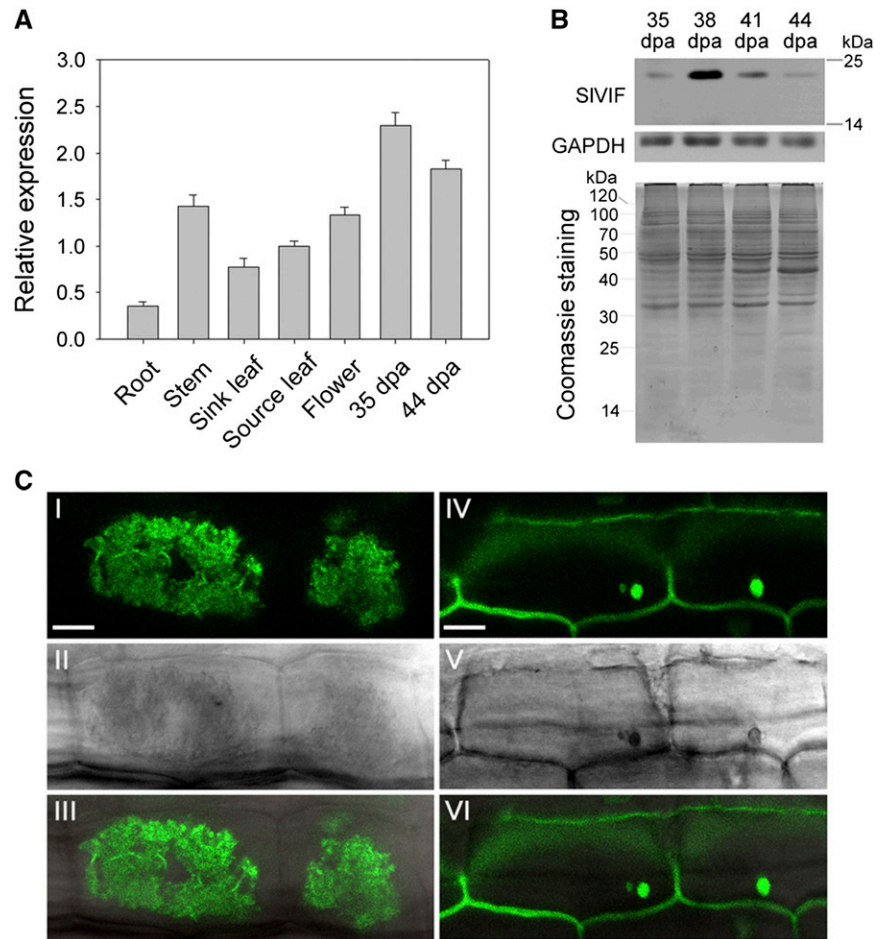
SlVIF silenced line 4 (S4) lines with the highest and lowest transcript level of *SlVIF*, respectively, were selected for further study.

Enzyme activity assays revealed that the VI activity was suppressed in fruit of the OE2 line but elevated in fruit of the S4 line, compared with wild-type fruit at different ripening stages (Fig. 6A). CWI and NI activities were not affected by presence of the transgenes (Fig. 6, B and C), confirming that SlVIF specifically inhibited VI activity. To investigate whether alteration of the SlVIF activity affected fruit sugar metabolism, levels of Suc, Glc, and Fru were measured. Overexpression of *SlVIF* resulted in 10-fold increase in Suc levels and a 40% decrease in hexose levels in 38-DPA OE2 fruits. In contrast, silencing *SlVIF* led to lower Suc levels and higher hexose levels than in the wild-type control fruit (Fig. 6, D–F). These results demonstrated that *SlVIF* influenced sugar metabolism and that altering its expression caused a substantial change in Suc levels in fruits.

We noted that alteration of Suc levels in the transgenic lines was accompanied by changes in the onset of fruit ripening (Fig. 6G). Fruit color changed from 35 DPA to 44 DPA in wild-type fruit, but the color transition from green to red was faster in the OE2 line

and slower in the S4 line (Fig. 6G). Moreover, we determined that while the red colored carotenoid pigment, lycopene, was detectable from 38 DPA in the wild-type fruit, it started to accumulate in the OE2 line at 35 DPA and continued to increase over time, whereas no significant changes in lycopene levels were observed from 35 DPA to 38 DPA in fruit of the S4 line (Fig. 6H). We concluded that altering sugar content affected carotenoid pigment biosynthesis, which in turn affected the timing of the onset of ripening. We also observed that overexpression of *SlVIF* led to a 60% increase of ethylene production at 35 DPA compared with the control, and repression of *SlVIF* expression resulted in significant reduction in ethylene production throughout the ripening process (Fig. 6I), suggesting that the altered sugar levels also affected phytohormone production to coordinately regulate fruit ripening.

To better understand the mechanism of action of *SlVIF* in ripening fruit, the transcript levels of a set of ripening-related marker genes (*RIN*, *NOR*, *LePG*, *EXP1*, *ACS2*, *ACO1*, *PSY1*, and *PDS*) were evaluated in *SlVIF*-overexpressing and -silenced tomato fruits by qRT-PCR (Fig. 7). The results indicated that the expression levels of these ripening marker genes were
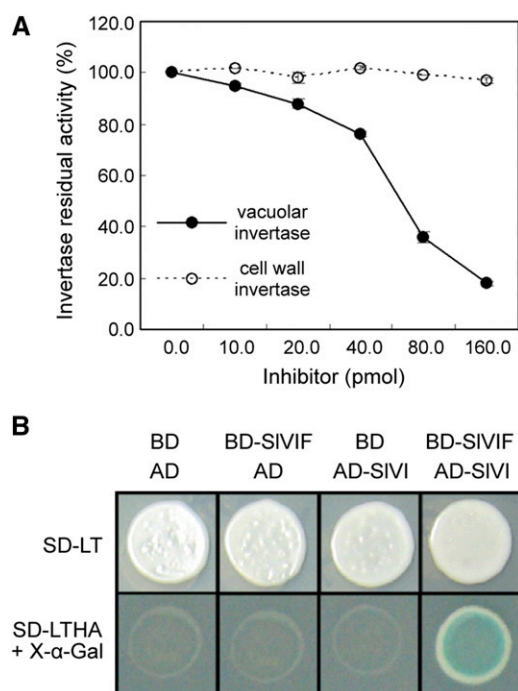
Figure 5. Interactions between SlVIF and SlVI. A, Inhibitory effects of recombinant SlVIF on tomato vacuolar invertase and cell wall invertase. Residual invertase activity was measured after preincubation with 10 to 160 pmol of recombinant SlVIF. Suc concentration in the assay was 20 mM. B, Interaction between SlVIF and SlVI in yeast. BD and AD represent plasmids pGBKT7 and pGADT7, respectively. Transformants were grown on selective medium SD-LT (SD/-Leu/-Trp) and SD-LTHA (SD/-Leu/-Trp/-His/-Ade) containing X-α-Gal for blue color development.

significantly influenced by *SlVIF*. Notably, the ripening regulators RIN and NOR were repressed in the *SlVIF* RNAi fruits at 38 DPA and 41 DPA but exhibited higher transcript levels at 44 DPA compared with the wild type. This suggests that gene expression of RIN and NOR was delayed in the *SlVIF* RNAi tomatoes during fruit ripening.

SlVIF Modulates the Expression of Ripening-Related Proteins

To further elucidate how *SlVIF* coordinately regulated fruit ripening, we performed an isobaric tags for relative and absolute quantification (iTRAQ)-based quantitative proteomic analysis of wild-type and *SlVIF* RNAi fruit. Proteins were extracted from the frozen pericarp tissue of wild-type and *SlVIF* RNAi fruits at 38 DPA and 41 DPA and labeled with 4-plex iTRAQ reagents (Fig. 8A). We analyzed three independent biological replicates, with a replicate corresponding to tissue pooled from fruits from five different plants for each stage and each genotype. Using a *S. lycopersicum* protein database (ftp://ftp.solgenomics.net/genomes/Solanum_lycopersicum/annotation/ITAG2.4_release/), a total of 4240, 4225, and 4381 proteins were identified in

both wild type and transgenic line in biological replicates 1, 2, and 3, respectively, with a global false discovery rate (FDR) <1% in each. A 2-fold cutoff led to the identification of 185 and 203 proteins with significantly altered levels in the *SlVIF* silenced fruits at 38 DPA and 41 DPA, respectively (Supplemental Table S6).

The differentially expressed proteins identified at 38 DPA and 41 DPA were categorized using Blast2go (https://www.blast2go.com/) into fourteen functional categories (Fig. 8B). Overall 139 of them were more abundant and 212 were less abundant, respectively, in the transgenic fruit than in wide type (Fig. 8C). We concluded that a set of ripening related proteins were significantly affected by *SlVIF* expression (Fig. 9). These included proteins involved in carotenoid biosynthesis, such as phytoene desaturase (PDS), in ethylene synthesis, such as ACC oxidase 1 (ACO1) and peptide Met sulfoxide reductase msrA (E4), and in cell wall degradation, such as polygalacturonase A (LePG) and pectinesterase (PME). To determine whether the protein expression patterns correlated with transcript levels, qRT-PCR was carried out for the corresponding genes using gene specific primers (Supplemental Table S7). Of the 15 genes analyzed, the expression of 12, including *PDS*, *CRTISO*, *ACO1*, *E4*, and *LePG*, were consistent with the protein abundance variations (Fig. 9). These results further indicated that *SlVIF* affected the expression of ripening-related genes.

DISCUSSION

RIN Regulates Expression of Genes Involved in Suc Metabolism

Given the importance of the ripening process in determining the quality, taste, and aroma of fruit, considerable effort had been focused on understanding its control (Klee and Giovannoni, 2011; Ecker, 2013). The MADS-box transcription factor, RIN, has been shown to be a global regulator of fruit ripening (Vrebalov et al., 2002; Martel et al., 2011) and to be critical for the production of characteristic tomato aromas derived from the LOX pathway (Qin et al., 2012). However, the particular genes related to sugar metabolism and their specific modulation by RIN have not been well defined. The VI, VIF, SS, HK, FK, and SPS gene families have been shown to be involved in Suc metabolism by regulating the degradation and resynthesis of Suc (Carrari and Fernie, 2006). Here, we identified a total of 36 genes involved in Suc metabolism in tomato (Supplemental Table S1) and analyzed their expression in the wild type and the *rin* mutant by qRT-PCR using gene specific primers (Fig. 1). Many of these genes were differentially expressed in the *rin* mutant compared with the wild type at equivalent DPA, including 11 invertase genes (*LIN5–9*, *VI*, *NI1–5*), a VI inhibitor gene (*VIF*), six Suc synthase genes (*SS1*, *SS3*, *SS4*, *SS5*, *SS6*, and *SS7*), four Suc phosphate synthase genes (*SPSA1–SPSC*), and six hexokinase genes (*HK1–6*). The data suggest that RIN regulates Suc metabolism during ripening by modulating the expression of a specific set of genes that play crucial roles in Suc degradation and resynthesis.
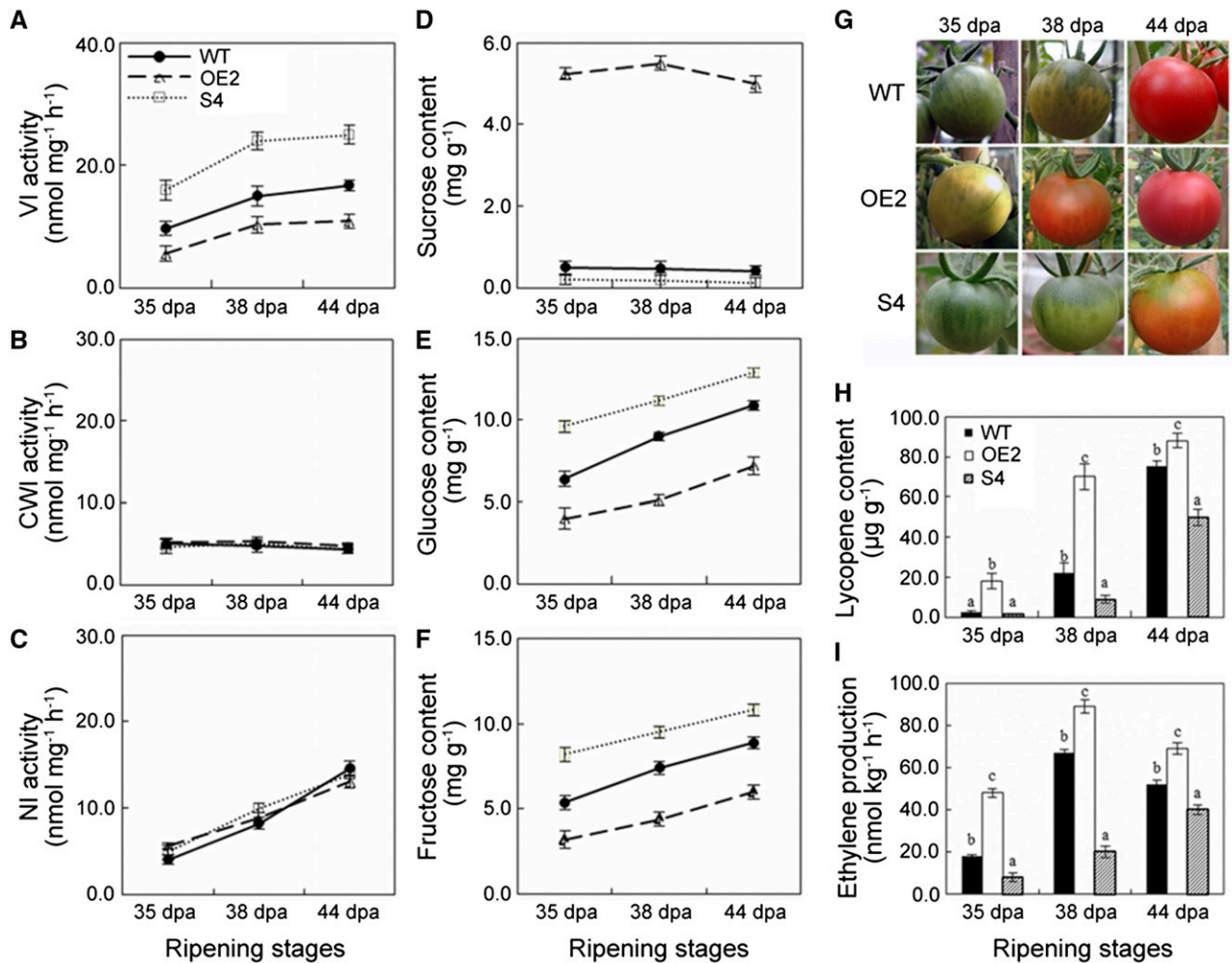
Figure 6. Function of tomato *SlVIF* in Suc metabolism and fruit ripening. Invertase activity, sugar content, color change phenotype, lycopene content, and ethylene production in fruit of *SlVIF* overexpressing line 2 (OE2), *SlVIF*-silenced line 4 (S4), and the wild type (WT) were examined during fruit ripening. A, Vacuolar invertase (VI) activity. B, Cell wall invertase (CWI) activity. C, Neutral invertase (NI) activity. D, Suc content. E, Glc content. F, Fru content. G, Photos of fruit from transgenic lines and wild-type control. H, Lycopene content. I, Ethylene production. Bars represent standard deviations of three biological replicates.

Sugars have important hormone-like functions as primary messengers in signal transduction in addition to their essential roles as substrates in the carbon and energy metabolism and in polymer biosynthesis (Rolland et al., 2002). Following Suc degradation by SS and VI, the resulting hexoses undergo phosphorylation by FK and HK for further metabolism (Claeyssen and Rivoal, 2007), suggesting that FK and HK are important in hexose metabolism, hexose sensing, and signaling (Eveland and Jackson, 2012). In this study, we showed that *RIN* governs sugar metabolism via the regulation of a number of genes, including *SlVI* and *SlVIF*, in the Suc synthesis and degradation pathway (Fig. 1B). *SlVI* expression was lower in the *rin* mutant while that of *SlVIF* was higher, suggesting that RIN can modulate Suc degradation during fruit ripening via promoting *SlVI* expression and suppressing its inhibitor *SlVIF*. Interestingly, the

expression of RIN changed substantially in the *SlVIF* RNAi tomatoes during fruit ripening (Fig. 7), suggesting that SlVIF affects *RIN* expression via a positive feed-back loop.

SlVIF Functions on Suc Metabolism and Lycopene Synthesis

The deduced SlVIF sequence was shown to share a high homology with vacuolar invertase inhibitors from tobacco and potato (Supplemental Figure S3). Four conserved Cys residues were identified that, in a potato vacuolar invertase inhibitor, have been shown to form disulfide bridges to stabilize the protein (Brummell et al., 2011). Gene expression analysis showed that *SlVIF* was expressed in both vegetative and reproductive organs (Fig. 4A) and that its expression increased in fruit from 35 DPA to 44 DPA (Fig. 4B), indicating
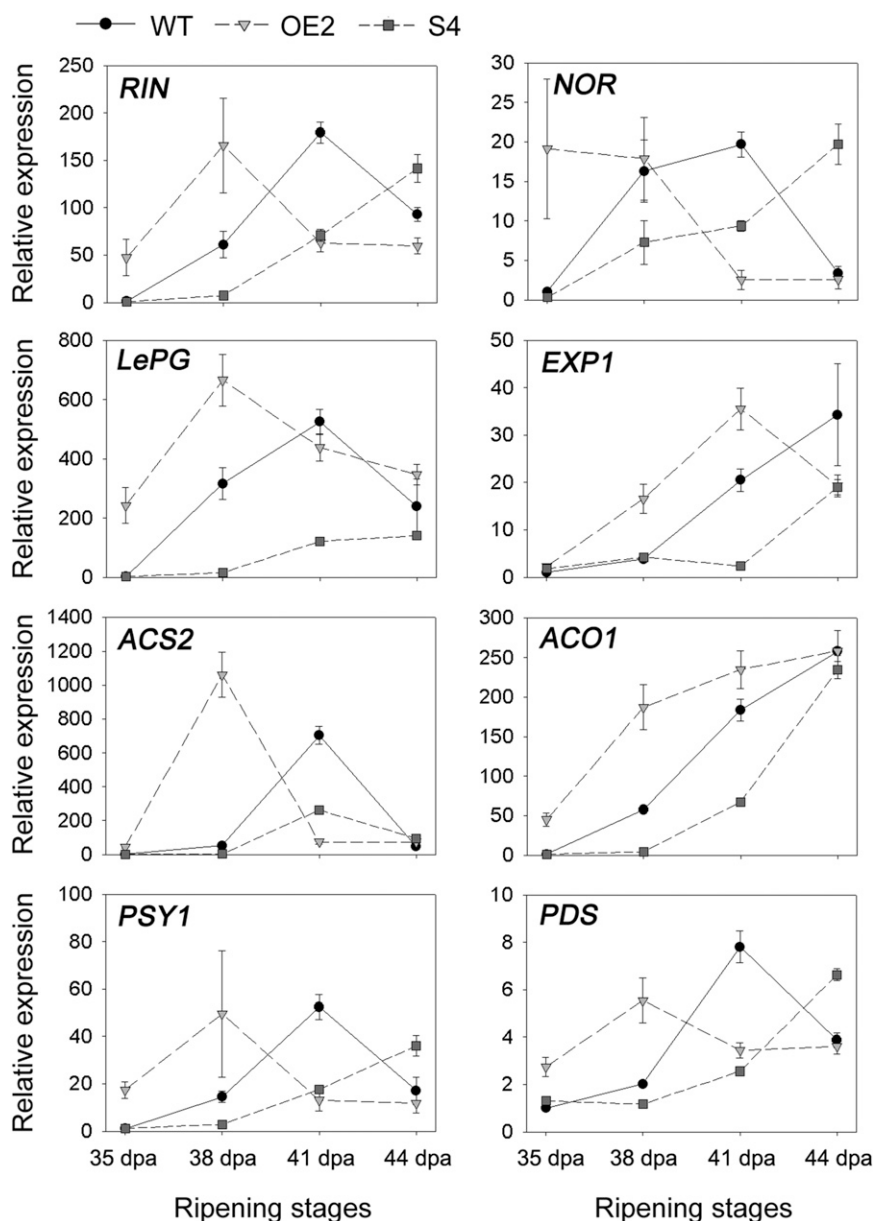
Figure 7. Expression of ripening marker genes in *SlVIF*-overexpressing and -silenced tomato fruits. The gene transcript levels were determined by qRT-PCR. Total RNA was extracted from pericarp tissues of *SlVIF*-overexpressing line 2 (OE2), *SlVIF*-silenced line 4 (S4), and the wild type (WT) at 35 DPA, 38 DPA, 41 DPA, and 44 DPA. The gene transcript levels are normalized against the *ACTIN* gene, followed by normalization against the wild type at 35 DPA. Values are means ± sd of three independent experiments. RIN, Ripening inhibitor; NOR, nonripening; LePG, polygalacturonase A; EXP1, expansin 1; ACS2, 1-aminocyclopropane-1-carboxylate synthase 2; ACO1, 1-aminocyclopropane-1-carboxylate oxidase; PSY1, phytoene synthase 1; PDS, phytoene desaturase.

that it is involved in fruit ripening. Greiner et al. (1999) suggested that the homologous protein from tobacco, NtVIF, is vacuolar, because overexpression of *NtVIF* in potato strongly inhibited VI but not CWI. This is consistent with our observation that recombinant GFP-SlVIF fusion protein accumulated in the vacuole of tomato root cells (Fig. 4C). Overexpression of *SlVIF* in tomato reduced the activity of VI, whereas silencing its expression resulted in increased VI activity (Fig. 6A), indicating that invertase activity is regulated by its endogenous inhibitor. Importantly, altered *SlVIF* expression did not affect the activities of CWI or NI (Fig. 6, B and C), demonstrating the specificity of SlVIF for SlVI. These results were further confirmed by Y2H analysis (Fig. 5B). Previous reports indicated a role for invertases and invertase

inhibitors in mediating sugar levels in plants (Greiner et al., 1999). Induction of the *VIF* expression in potato tubers contributes to cold-induced sweetening resistance due to its inhibition of VI and resulting decrease in the accumulation of reducing sugars (Brummell et al., 2011). Consistent with its predicted role, overexpression of *SlVIF* in tomato fruits significantly inhibited Suc hydrolysis, leading to an increase in Suc content and a reduction in hexose levels, while suppression of *SlVIF* promoted Suc hydrolysis and enhanced hexose levels (Fig. 6, D–F).

Posttranslational regulation of enzymes involved in the sugar metabolic pathway represents an important mechanism for regulating sugar levels and composition in plants (Koch, 2004). Moreover, posttranslational elevation of CWI activity by silencing of its inhibitor has
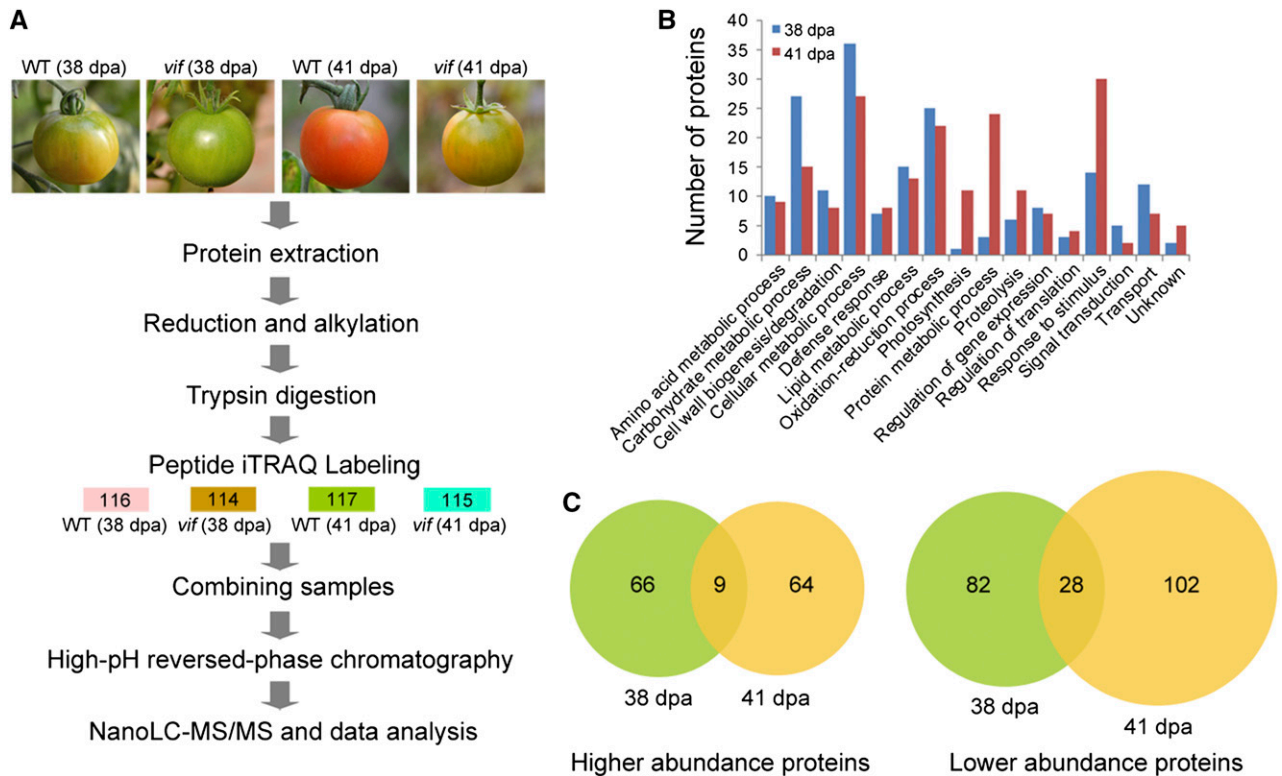
Figure 8. Identification of differentially expressed proteins in *SlVIF* silenced tomato fruits by iTRAQ-based quantitative proteomic analysis. A, Schematic diagram of the workflow used in this study. Three sets of biological replicate samples from wild-type (WT) and *SlVIF*-silenced fruit (*vif*) at 38 DPA and 41 DPA were analyzed by iTRAQ, using the NanoLC-MS/MS workflow for examining proteome changes. B, GO categories of differentially expressed proteins at 38 DPA or 41 DPA. C, Venn diagram of differentially expressed proteins identified at 38 DPA and 41 DPA. The numbers of differentially abundant proteins at each ripening stage are shown.

been shown to result in increased hexose accumulation in tomato fruits (Jin et al., 2009), and a number of studies have shown that VI activity is correlated with hexose levels in hexose-accumulating species of tomato (Miron and Schaffer 1991; Klann et al., 1996). External Suc supplementation was previously reported to promote a color break in citrus (*C. unshiu*) and tomato fruit (Iglesias et al., 2001; Télef N, et al., 2006), indicating a link between sugars and pigments. Color transition in tomato fruits is due to the degradation of chlorophylls and the simultaneous accumulation of carotenoids, mainly lycopene, which is affected by several factors (Giovannoni, 2004). However, evidence supporting a role for sugars in pigment synthesis and consequently fruit ripening in vivo is still lacking. In this study, overexpression of *SlVIF* in tomato decreased hexose content during ripening, in contrast to fruits from wild-type and *SlVIF* RNAi plants (Fig. 6, E and F), suggesting a connection between VI activity and hexose accumulation. Interestingly, altering Suc levels by modification of *SlVIF* expression resulted in a clear change in the timing of the onset of fruit ripening. Specifically, the red transition was faster in fruit of the *SlVIF*-overexpressing line, but slower in the *SlVIF* RNAi line compared with the wild-type fruit (Fig. 6G), indicating

that *SlVIF* plays a role in the regulation of Suc metabolism and pigment biosynthesis.

SlVIF Modulates Ethylene Production and the Expression of Ripening-Related Genes

Ethylene is thought to be required for the Suc-induced modulation of carotenoid accumulation in both climacteric and nonclimacteric fruit (Iglesias et al., 2001; Télef et al., 2006), and ethylene production is concomitant with color change and lycopene biosynthesis, which is an indicator of ripening in many climacteric fruit (Giovannoni, 2007). Suppression of acid invertase expression can stimulate ethylene production in tomato and muskmelon fruit (Klann et al., 1996; Yu et al., 2008), and we saw that overexpression of *SlVIF* in tomato increased ethylene production (Fig. 6I) and led to a precocious color shift, due to elevated lycopene accumulation (Fig. 6H). In contrast, ethylene production was decreased, and fruit coloring was delayed by silencing *SlVIF* in tomato (Fig. 6G). This suggests that *SlVIF* is involved in the regulation of ethylene production and fruit ripening. Using iTRAQ-based quantitative proteomic analysis, we identified 185 and
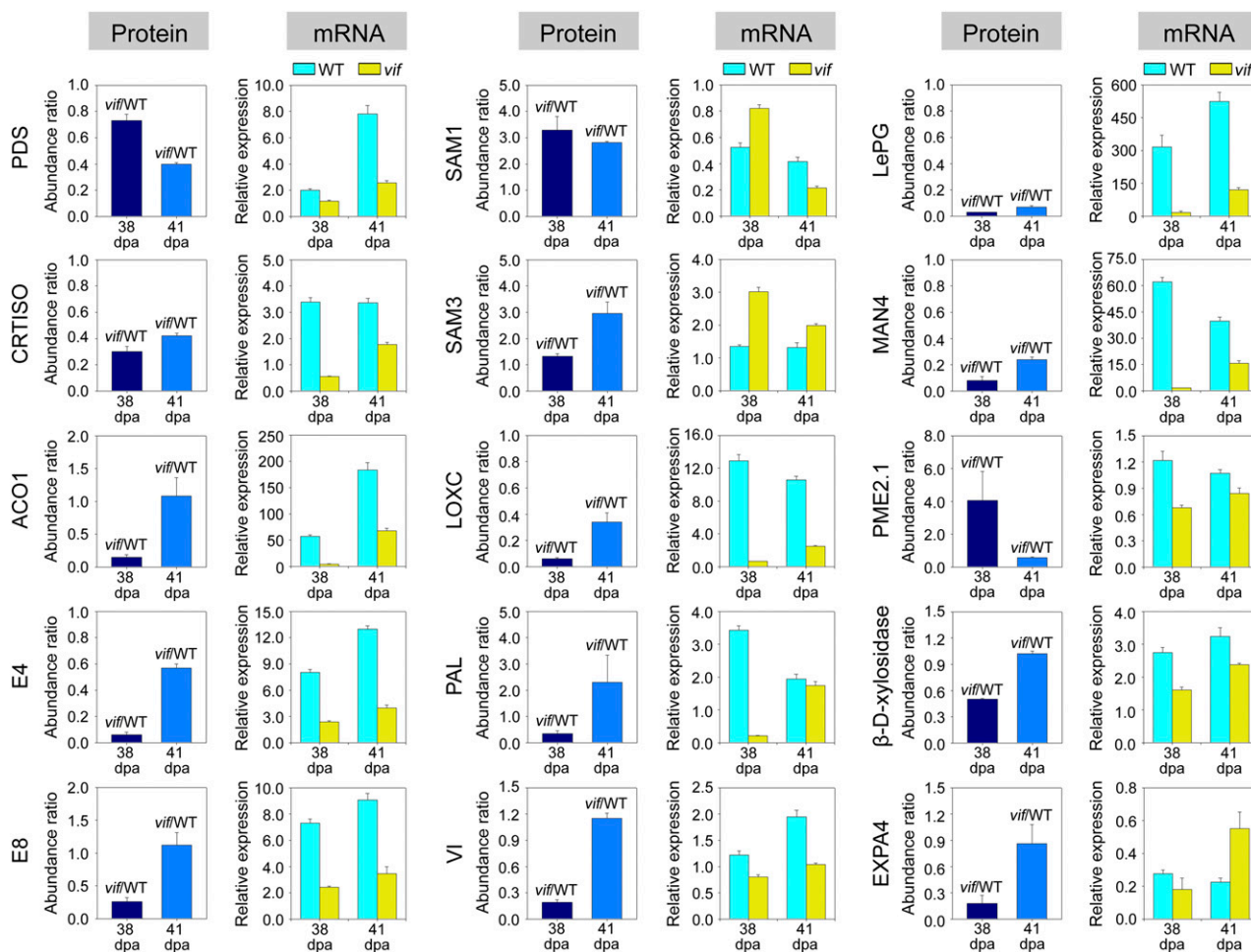
Figure 9. Quantitative proteomic analysis showing that ripening-related genes are affected by *SlVIF* expression. The changes in protein abundance in the *SlVIF*-silenced fruits (*vif*) at 38 DPA and 41 DPA are shown as the ratio between *vif* and the wild type (WT). The mRNA expression levels were measured by qRT-PCR. Total RNA was extracted from pericarp tissues of *SlVIF* silenced fruit (*vif*) and the wild type at 35 DPA, 38 DPA, 41 DPA, and 44 DPA. The gene transcript levels were normalized against the *ACTIN* gene, followed by normalization against the wild type at 35 DPA. The changes in transcript levels at 38 DPA and 41 DPA are shown. The results for both protein and mRNA expression are means ± sd from three independent experiments. PDS, Phytoene desaturase; CRTISO, carotenoid isomerase; ACO1, 1-aminocyclopropane-1-carboxylate oxidase; E4, peptide Met sulf-oxide reductase; E8, 1-aminocyclopropane-1-carboxylate oxidase-like protein; SAM1, *S*-adenosyl-Met synthase 1; SAM3, *S*-adenosyl-Met synthase 3; LoxC, lipoxygenase; PAL, Phe ammonia-lyase; VI, vacuolar invertase; LePG, polygalacturonase A; MAN4, mannan endo-1,4-*β*-mannosidase; PME2.1, pectinesterase; EXPA4, expansin.

203 proteins whose abundance was significantly different in *SlVIF*-silenced fruit compared with wild-type fruit at 38 DPA and 41 DPA, respectively (Fig. 8). Of these, 139 were more abundant in the transgenic fruit and 212 were less abundant (Fig. 8C). Suppression of *SlVIF* expression affected the abundance of many ripening-related proteins (Fig. 9), including PDS, ACO1, E4, and LePG. qRT-PCR analysis indicated that the expression levels of several ripening-related genes (*PDS*, *ACO1*, *E4*, and *LePG*) were consistent with the corresponding protein abundance variations (Fig. 9). Altering sugar content and/or *SlVIF* expression also affected the abundance of other ripening-related genes, suggesting a potential role for *SlVIF* in the regulation of

fruit ripening. Finally, ChIP-qPCR and EMSA assays showed that RIN directly bound to the promoters of *SlVI* and *SlVIF*, along with those of 14 other genes involved in Suc metabolism (Figs. 2 and 3; Supplemental Fig. S2). These results indicate that RIN controls sugar metabolism by modulating the expression of genes involved in Suc synthesis and degradation.

In conclusion, our study highlights an important role for *SlVIF* in fruit ripening and establishes a link between Suc metabolism, lycopene synthesis, and ripening in tomato fruit. Our results further suggest that *SlVIF* has potential value as a genetic tool to regulate tomato fruit ripening through manipulating the interaction of VI and its inhibitor.

MATERIALS AND METHODS

Plant Materials and Growth Conditions

Tomato (*Solanum lycopersicum* cv Ailsa Craig) plants were grown at 25°C with a 16-h photoperiod. The flowers were tagged at anthesis to determine ripening stages. For plants grown in vitro, seeds were germinated on Murashige and Skoog medium (Murashige and Skoog, 1962) with 16 h of light at 25°C and 8 h of darkness at 22°C. Seeds of the tomato mutant *rin* in the 'Ailsa Craig' background were kindly provided by Dr. James J. Giovannoni (Boyce Thompson Institute for Plant Research, Cornell University, Ithaca, NY). Fruit ripening stages used in this study were 35, 38, 41, and 44 DPA. Fruits of *rin* or transgenic lines were collected at the equivalent ripening stages determined by the number of DPA.

Identification of Tomato Genes Involved in Suc Metabolism

In order to identify tomato orthologs of genes involved in Suc metabolism (i.e. genes encoding invertases, invertase inhibitors, Suc synthases, Suc phosphate synthases, fructokinases, and hexokinases), BLAST searches were carried out against the National Center for Biotechnology Information (http://www.ncbi. nlm.nih.gov/) and SGN (http://solgenomics.net/) databases using the reported gene sequence as a query. The uniqueness of the identified genes was manually verified to remove redundant sequences. GENSCAN (http://genes. mit.edu/GENSCAN.html) was used to predict the putative open reading frames and protein sequences.

qRT-PCR

Total RNA (2 μg) was extracted from pericarp tissues as described by Moore et al. (2005). The extracted RNA was treated with DNase (Promega) and reverse-transcribed using an oligo(dT)$_{18}$ primer with Moloney murine leukemia virus reverse transcriptase (Promega) to synthesize cDNA. qRT-PCR was performed with Takara SYBR Green Master Mix and gene-specific primers in a volume of 20 μL using an Mx3000P system (Stratagene). The following condition was applied for PCR amplification: 95°C for 10 min, followed by 40 cycles of 95°C for 15 s and 60°C for 30 s. *ACTIN* (BT012695) was used as an internal control, and the relative expression was calculated using the comparative $2^{(-\Delta Ct)}$ method (Schmittgen and Livak, 2008). Each experiment had three biological repeats, each with three technical replicates.

ChIP Assay

ChIP assays were performed as described previously (Qin et al., 2012). Pericarp tissue from 41 DPA fruit was collected and submerged in 1% formaldehyde under a vacuum to cross-link genomic DNA and protein. Nuclei were enriched and then sonicated in nuclei lysing buffer containing 50 mM Tris-HCl, pH 8.0, 10 mM EDTA, 1% SDS, 0.1 mM phenylmethylsulfonyl fluoride, and proteinase inhibitors. The conditions for sonication were optimized to shear DNA to an average size of 500 ~ 1000 bp. A small aliquot of sonicated chromatin was reversely cross-linked and served as the input DNA control. The remaining chromatin sample was centrifuged at 16,000g for 5 min at 4°C, and the supernatant was diluted 10-fold in ChIP dilution buffer (1.1% Triton X-100, 1.2 mM EDTA, 16.7 mM Tris-HCl, pH 8.0, 167 mM NaCl, 0.1 mM phenylmethylsulfonyl fluoride, and proteinase inhibitors). Protein A-agarose/salmon sperm DNA beads (Millipore) were used to preclear the chromatin solution for 1 h at 4°C. Immunoprecipitation was carried out with affinity-purified RIN polyclonal antibody (see below), and the tube containing the samples were incubated on a rotator with gentle agitation (25 rpm) for 12 h at 4°C. Reactions with preimmune serum IgG and without antibody were used as negative and mock controls, respectively. Protein-chromatin immunocomplexes were captured on Protein A-agarose beads by incubating at 4°C for 1 h. The beads were collected by centrifugation at 16,000g for 2 min at 4°C, and the bead-bound immunocomplexes were eluted with elution buffer (1% SDS, 0.1 M NaHCO$_3$) by gently rotating for 15 min at 65°C. The beads were collected and the supernatant (eluate) was transferred to a fresh tube. The cross linking of immunoprecipitated DNA was then reversed by incubation of the eluate in 0.2 M NaCl at 65°C overnight. The immunoprecipitated DNA was purified after Proteinase K (Invitrogen) treatment and eluted in TE buffer (10 mM Tris-HCl, pH 8.0, 1 mM EDTA) before being used for PCR using the same conditions as for qRT-PCR analysis. The RIN binding sites (CArG box) in the promoters of selected genes

were analyzed using PLACE Web Signal Scan (http://www.dna.affrc.go.jp/ PLACE/signalup.html). Primers used for PCR amplification are listed in Supplemental Table S4.

EMSA

Recombinant His-tagged RIN protein was expressed in *Escherichia coli* and purified as described previously (Qin et al., 2012). The binding activity of RIN to specific DNA sequences was assayed using a Lightshift Chemiluminescent EMSA kit (Thermo Scientific). Briefly, purified RIN protein (1 μg) in a binding buffer containing 10 mM Tris-HCl, pH 7.2, 50 mM KCl, 1 mM dithiothreitol 2.5% glycerol, 0.05% NP-40, and 50 ng μL^{-1} polydeoxy (inosinate-cytidylate) was incubated for 20 min at room temperature in the presence or absence of unlabeled (double-stranded) competitor probes. The 3' biotin end-labeled dsDNA probes, which were constructed by annealing complementary oligonucleotides, were then added, and the incubation continued for 20 min. The sequences of the biotin-labeled probes, are listed in Supplemental Table S5. Protein-DNA complexes were separated on 6% native polyacrylamide gels, and the biotin-labeled probes were detected according to the instructions provided with the EMSA kit.

Recombinant Protein Expression and Antibody Preparation

Recombinant RIN protein was prepared as described previously (Qin et al., 2012). For recombinant SlVIF protein preparation, a *SlVIF* gene fragment without the predicted putative vacuolar sorting sequence (SignalP 4.0) was amplified from tomato cDNA using primers *SlVIF*-F (5'-GGTACCAACAA-CAACAACAACATCAT-3') and *SlVIF*-R (5'-GAGCTCTCATAATAACATTC-TAATTA-3'). The fragments were digested using *Kpn*I and *Sac*I and inserted into the pET30a vector (Merck). The resulting plasmid was transformed into *E. coli* BL21 (Lys) cells, and expression of the recombinant protein was induced by 1 mM of isopropyl-β-D-thiogalacto-pyranoside. Recombinant His-tagged proteins were purified using Ni-NTA His-Bind resin (Merck).

Antibodies were raised against the recombinant RIN and SlVIF proteins in New Zealand white rabbits by AbMax Biotechnology. Polyclonal antibodies were affinity purified from antisera using AminoLink Plus coupling resin, according to the manufacturer's instructions (Thermo Scientific).

Western Blot Analysis

Proteins were extracted from tomato fruit harvested at different ripening stages as in Bate et al. (2004), fractionated on a 12% SDS-PAGE gel and electrotransferred to an Immobilon-P polyvinylidene difluoride membrane (Millipore). The membranes were blocked at 20°C for 2 h with 5% bovine serum albumin in PBS-Tween buffer (137 mM NaCl, 2.7 mM KCl, 8.1 mM NaH$_2$PO$_4$, 1.5 mM KH$_2$PO$_4$, and 0.1% Tween 20, pH 7.4). Immunoblots were performed at 4°C overnight with affinity-purified rabbit polyclonal anti-SlVIF as described by Wang et al. (2014). The membranes were washed with PBS-Tween (3 × 10 min) and treated with the corresponding secondary antibodies (Abmart; 1:5000 dilutions) conjugated to horseradish peroxidase. Immunoreactive bands were visualized using a chemiluminescence detection kit (SuperSignal, Pierce Biotechnology). As a protein control, an anti-glyceraldehyde-3-phosphate dehydrogenase (Abmart) immunoblot was used. Additionally, Coomassie Brilliant Blue staining was used as a loading control.

Plasmid Construction and Plant Transformation

To construct the 35S:GFP:*SlVIF* vector, the full-length *SlVIF* cDNA was inserted into a GFP expression vector pCAMBIA2300. The SlVIF overexpression construct was made by cloning the full-length SlVIF cDNA into the pBI121 vector (kindly provided by Dr. Jing Bo Jin from Institute of Botany, the Chinese Academy of Sciences, Beijing) downstream of the 35S promoter.

To construct the *SlVIF* RNAi plasmid, a 285-bp *SlVIF* fragment was amplified from tomato cDNA (prepared from fruit pericarp at 35 DPA as described above) by the primer pair 5'-TATAACACCGTCCTACGAGCCG-3' and 5'-TCTTTATATCTGGTTCACGTAACG-3'. The resulting product was cloned into the PCR8/GW/TOPO Gateway entry vector (Invitrogen). The cloned fragment was subsequently transferred into the destination vector pK7GWIWG2 (Karimi et al., 2002) using the LR Clonase II enzyme (Invitrogen) according to the manufacturer's instructions.

The above constructs were individually transformed into *Agrobacterium tumefaciens* strain GV3101 by electroporation. Tomato transformation was performed according to Fillatti et al. (1987). The presence of transgenes in kanamycin-resistant plants was confirmed by PCR using a forward primer corresponding to the 35S promoter and a reverse primer specific for *SlVIF*: 5′-CGGAAACCTCCTCG-GATTCCATT-3′ and 5′-GGCTACCGTTACATCGGCTCGTA-3′.

Invertase Activity and Inhibition Assays

The activities of VI, CWI, and NI were assayed according to Miron and Schaffer (1991) and Klann et al. (1993). Approximately 2 g of pericarp was homogenized in 10 mL of extraction buffer containing 50 mM HEPES-NaOH, pH 7.5, 5 mM MgC1₂, 1 mM EDTA, 2.5 mM dithiothreitol, 10 mM ascorbic acid, and 5% polyvinylpolypyrrolidone. After centrifugation at 20,000g for 30 min at 4°C, the supernatants were dialyzed for 16 h against 25 mM HEPES-NaOH, pH 7.5, and 0.5 mM EDTA and used as a crude enzyme extract for VI and NI activity assays. The insoluble pellet was washed three times with extraction buffer and extracted for 1 h with 10 mL of extraction buffer containing 1 M NaCl. After centrifugation at 20,000g for 30 min at 4°C, the supernatants were dialyzed overnight and used as crude enzyme extract for CWI assays. For VI and CWI activity assays, 0.2 mL of enzyme extract was incubated for 30 min at 37°C with 0.6 mL of 100 mM sodium acetate, pH 4.8, and 0.2 mL of 100 mM Suc. Reactions were stopped by placing the reaction tubes in boiling water for 5 min and reducing sugars were measured using dinitrosalicylic acid (Sumner, 1921). NI activity was assayed in 50 mM HEPES-NaOH, pH 7.5, instead of sodium acetate, pH 4.8.

For inhibition studies, VI or CWI enzyme preparations were mixed with recombinant SlVIF protein and incubated in the assay buffer for 30 min at 37°C prior to addition of Suc and measurement of enzyme activity.

Y2H Assay

To generate the vector system for the Y2H analysis, the *SlVIF* cDNA fragment encoding the mature protein and the full-length cDNA of *SlVI* (GenBank accession no. M81081) were cloned into the pGBKT7 (BD) and pGADT7 (AD) vectors (Clontech), using specific primers (*SlVIF*: 5′-CGGAATT-CAACAACAACAACAACATCAT-3′ and 5′-AACTGCAGTCATAATAACA-TTCTAATTATG-3′; *SlVI*: 5′-CGGAATTCATGGCCACTCAGTGTTATGA-3′ and 5′-CCGCTCGAGTTACAAGTCTTGCAAAGGGA-3′), resulting in the BD-SlVIF and AD-SlVI plasmids. The two plasmids were cotransformed into the yeast strain *Saccharomyces cerevisiae* AH109 according to the manufacturer's instructions (Clontech) and dripped on synthetic dropout nutrient medium SD-LT (SD/-Leu/-Trp) and SD-LTHA (SD/-Leu/-Trp/-His/-Ade) containing X-α-Gal. As a control, BD and AD, BD-SlVIF and AD, and BD and AD-SlVI were also cotransformed and analyzed, respectively.

Sugar, Lycopene, and Ethylene Measurements

Sugars were extracted and determined according to Zhu et al. (2013).

Pericarp lycopene content was measured as described by Choi and Huber (2008). Tomato pericarp tissue samples (5 g) were homogenized for 1 min in 50 mL of hexane-acetone-ethanol (2:1:1, v/v) wrapped in aluminum foil to exclude light, then 15 mL of water was added and the samples were vortexed for 10 s. After allowing phase separation on ice, the lycopene concentration was determined by measuring the absorbance of the organic phase (hexane) at 503 nm. The lycopene content was calculated using the molar extinction coefficient of 17.2 L mol⁻¹ m⁻¹ and expressed as μg g⁻¹ fresh weight. Three independent samples derived from five fruits at each ripening stage were used for lycopene measurements.

Ethylene production was determined according to Zhu et al. (2010). Fruit were harvested at different ripening stages, weighed, and transferred to 1 L gastight jars. The jars were sealed and incubated at 25°C for 2 h, then 1 mL of gas sample was withdrawn from the headspace with a syringe and injected into a gas chromatograph (SQ-206, Beifen-Ruili Analytical Instrument Company), equipped with an activated alumina column and a flame ionization detector. Three independent samples derived from five fruits at each ripening stage were used for the ethylene measurements.

Protein Isolation, iTRAQ Labeling, and NanoLC-Tandem Mass Spectrometry Analysis

Fruits were harvested at 38 DPA and 41 DPA, and total cellular protein was extracted from fruit pericarp tissue as described by Saravanan and Rose (2004).

Proteins were solubilized in a protein buffer consisting of 500 mM triethy-lammonium bicarbonate and 0.6% (w/v) SDS, pH 8.5, and the protein concentrations were determined by the Bradford method (Bradford, 1976) with bovine serum albumin as a standard. Proteins from each sample were reduced with 10 mM tris-(2-carboxyethyl)phosphine, alkylated with 50 mM methyl methanethiosulfonate, and digested with 10 ng μL⁻¹ trypsin using the filter-aided sample preparation method (Wiśniewski et al., 2009). The tryptic peptides were labeled using the iTRAQ Reagents 4-plex kit (Applied Biosystems) according to the manufacturer's protocol. Samples taken from wild-type and *SlVIF*-silenced tomatoes at 38 DPA were labeled with iTRAQ tags 116 and 114, respectively, while samples from wild-type and *SlVIF*-silenced tomatoes at 41 DPA were labeled with iTRAQ tags 117 and 115, respectively. Three independent biological replicates were analyzed. The iTRAQ-labeled samples were combined and then fractionated with high-pH reversed-phase chromatography using the Agilent Technologies 1290 UPLC system. Briefly, the pooled iTRAQ-labeled peptides were reconstituted using buffer A (20 mM ammonium formate, pH 10, in water) and loaded onto a 4.6 × 250 mm, 150 Å size Durashell C18 (L) column containing 5 μm particles (Agela Technologies). The peptides was eluted at a flow rate of 0.8 ml min⁻¹ with a gradient of 2% buffer B (20 mM ammonium formate in 80% acetonitrile, pH 10) for 5 min, 2% to 30% buffer B for 25 min, and 30% to 90% buffer B for 10 min. The system was maintained in 90% buffer B for 10 min and then equilibrated with 2% buffer B for 10 min. The elution was monitored by measuring UV A_{210}, and fractions were collected every 1 min. A total of 48 fractions were collected and pooled into a total of six fractions. After reconstitution in formic acid, the labeled peptides were desalted and submitted for NanoLC-tandem mass spectrometry (MS/MS) analysis.

The MS analysis was carried out using a NanoLC system (NanoLC-2D Ultra Plus, Eksigent) equipped with a Triple TOF 5600 Plus mass spectrometer (AB SCIEX). The iTRAQ-labeled peptide mixtures were desalted on a 100 μm × 20 mm trap column and eluted on an analytical 75 μm × 150 mm column. Both the trap column and the analytical column were filled with the Magic C18-AQ 5 μm 200 Å phase (Michrom Bioresources). Peptides were separated by a gradient formed by 0.1% formic acid (mobile phase A) and 100% acetonitrile, 0.1% formic acid (mobile phase B), from 5% to 30% of mobile phase B over 75 min at a flow rate of 300 nL/min. The precursor ions were selected across the mass range of 350 to 1500 m/z. High-resolution mode (>30,000) was applied using 250 ms accumulation time per spectrum. A maximum of 25 precursors per cycle from each MS spectrum were chosen for fragmentation with 100 ms minimum accumulation time for each precursor and dynamic exclusion for 18 s. Tandem mass spectra were recorded in high-sensitivity mode (resolution >15,000) with rolling collision energy and iTRAQ reagent collision energy adjustment on.

Protein identification and quantification were performed using ProteinPilot 4.5 software (AB SCIEX), and database searches were carried out using the *S. lycopersicum* protein database ITAG2.4_proteins_full_desc.fasta (ftp://ftp.solgenomics.net/genomes/Solanum_lycopersicum/annotation/ITAG2.4_release/). The following parameters was applied: (1) sample type: iTRAQ 4-plex (peptide labeled); (2) Cys alkylation: MMTS; (3) digestion: trypsin; (4) instrument: TripleTOF 5600; (5) species: none; (6) quantitate: yes; (7) bias correction: yes; (8) background correction: yes; (9) search effort: thorough; and (10) FDR analysis: yes. The peptide for quantification was automatically chosen by the Pro Group algorithm (AB SCIEX) to calculate the reporter peak area. The reverse database search method (Elias and Gygi, 2007) was used to estimate the global FDR for peptide identification. Proteins identified below the 1% global FDR were used to calculate the meaningful cutoff value with the experimental replicate method (Gan et al., 2007).

Accession Numbers

Sequence data from this article can be found in the GenBank/EMBL data libraries under accession number KC007445.

Supplemental Data

The following supplemental materials are available.

Supplemental Figure S1. The binding ability of RIN to the promoter of *ACS2* as revealed by chromatin immunoprecipitation.

Supplemental Figure S2. Chromatin immunoprecipitation reveals the direct binding of RIN to the promoters of genes involved in Suc metabolism.

Supplemental Figure S3. Alignment of amino acid sequences of invertase inhibitors from various plants.

Supplemental Table S1. Genes involved in Suc metabolism.

Supplemental Table S2. Primers used in qRT-PCR analysis of Suc metabolism genes.

Supplemental Table S3. Ripening marker genes used for qRT-PCR analysis in this study.

Supplemental Table S4. Gene-specific primers used in ChIP-qPCR assay.

Supplemental Table S5. Primers used for probes of EMSA.

Supplemental Table S6. Identification of the differentially expressed proteins in the *SlVIF* silenced tomato fruit (*vif*) using iTRAQ-based quantitative proteomic analysis.

Supplemental Table S7. Primers for qRT-PCR analysis of selected genes identified in iTRAQ.

ACKNOWLEDGMENTS

LITERATURE CITED

Alba R, Payton P, Fei Z, McQuinn R, Debbie P, Martin GB, Tanksley SD, Giovannoni JJ (2005) Transcriptome and selected metabolite analyses reveal multiple points of ethylene control during tomato fruit development. Plant Cell **17:** 2954–2965

Bate NJ, Niu X, Wang Y, Reimann KS, Helentjaris TG (2004) An invertase inhibitor from maize localizes to the embryo surrounding region during early kernel development. Plant Physiol **134:** 246–254

Borsani J, Budde CO, Porrini L, Lauxmann MA, Lombardo VA, Murray R, Andreo CS, Drincovich MF, Lara MV (2009) Carbon metabolism of peach fruit after harvest: changes in enzymes involved in organic acid and sugar level modifications. J Exp Bot **60:** 1823–1837

Bradford MM (1976) A rapid and sensitive method for the quantitation of microgram quantities of protein utilizing the principle of protein-dye binding. Anal Biochem **72:** 248–254

Brummell DA, Chen RK, Harris JC, Zhang H, Hamiaux C, Kralicek AV, McKenzie MJ (2011) Induction of vacuolar invertase inhibitor mRNA in potato tubers contributes to cold-induced sweetening resistance and includes spliced hybrid mRNA variants. J Exp Bot **62:** 3519–3534

Carrari F, Fernie AR (2006) Metabolic regulation underlying tomato fruit development. J Exp Bot **57:** 1883–1897

Choi ST, Huber DJ (2008) Influence of aqueous 1-methylcyclopropene concentration, immersion duration, and solution longevity on the postharvest ripening of breaker-turning tomato (Solanum lycopersicum L.) fruit. Postharvest Biol Technol **49:** 147–154

Claeyssen E, Rivoal J (2007) Isozymes of plant hexokinase: occurrence, properties and functions. Phytochemistry **68:** 709–731

Davies C, Robinson SP (1996) Sugar accumulation in grape berries. Cloning of two putative vacuolar invertase cDNAs and their expression in grapevine tissues. Plant Physiol **111:** 275–283

Ecker JR (2013) Epigenetic trigger for tomato ripening. Nat Biotechnol **31:** 119–120

Elias JE, Gygi SP (2007) Target-decoy search strategy for increased confidence in large-scale protein identifications by mass spectrometry. Nat Methods **4:** 207–214

Elliott KJ, Butler WO, Dickinson CD, Konno Y, Vedvick TS, Fitzmaurice L, Mirkov TE (1993) Isolation and characterization of fruit vacuolar invertase genes from two tomato species and temporal differences in mRNA levels during fruit ripening. Plant Mol Biol **21:** 515–524

Eveland AL, Jackson DP (2012) Sugars, signalling, and plant development. J Exp Bot **63:** 3367–3377

Fraser PD, Truesdale MR, Bird CR, Schuch W, Bramley PM (1994) Carotenoid biosynthesis during tomato fruit development (evidence for tissue-specific gene expression). Plant Physiol **105:** 405–413

Fillatti JJ, Kiser J, Rose R, Comai L (1987) Efficient transfer of a glyphosate tolerance gene into tomato using a binary Agrobacterium tumefaciens vector. Nat Biotechnol **5:** 726–730

Fridman E, Carrari F, Liu YS, Fernie AR, Zamir D (2004) Zooming in on a quantitative trait for tomato yield using interspecific introgressions. Science **305:** 1786–1789

Fridman E, Zamir D (2003) Functional divergence of a syntenic invertase gene family in tomato, potato, and Arabidopsis. Plant Physiol **131:** 603–609

Fujisawa M, Nakano T, Shima Y, Ito Y (2013) A large-scale identification of direct targets of the tomato MADS box transcription factor RIPENING INHIBITOR reveals the regulation of fruit ripening. Plant Cell **25:** 371–386

Gan CS, Chong PK, Pham TK, Wright PC (2007) Technical, experimental, and biological variations in isobaric tags for relative and absolute quantitation (iTRAQ). J Proteome Res **6:** 821–827

German MA, Asher I, Petreikov M, Dai N, Schaffer AA, Granot D (2004) Cloning, expression and characterization of *LeFRK3*, the fourth tomato (*Lycopersicon esculentum* Mill.) gene encoding fructokinase. Plant Sci **166:** 285–291

German MA, Dai N, Chmelnitsky I, Sobolev I, Salts Y, Barg R, Schaffer AA, Granot D (2002) *LeFRK4*, a novel tomato (*Lycopersicon esculentum* Mill.) fructokinase specifically expressed in stamens. Plant Sci **163:** 607–613

Giovannoni JJ (2004) Genetic regulation of fruit development and ripening. Plant Cell (Suppl) **16:** S170–S180

Giovannoni JJ (2007) Fruit ripening mutants yield insights into ripening control. Curr Opin Plant Biol **10:** 283–289

Godt DE, Roitsch T (1997) Regulation and tissue-specific distribution of mRNAs for three extracellular invertase isoenzymes of tomato suggests an important function in establishing and maintaining sink metabolism. Plant Physiol **115:** 273–282

Goren S, Huber SC, Granot D (2011) Comparison of a novel tomato sucrose synthase, SlSUS4, with previously described SlSUS isoforms reveals distinct sequence features and differential expression patterns in association with stem maturation. Planta **233:** 1011–1023

Greiner S, Krausgrill S, Rausch T (1998) Cloning of a tobacco apoplasmic invertase inhibitor. Proof of function of the recombinant protein and expression analysis during plant development. Plant Physiol **116:** 733–742

Greiner S, Rausch T, Sonnewald U, Herbers K (1999) Ectopic expression of a tobacco invertase inhibitor homolog prevents cold-induced sweetening of potato tubers. Nat Biotechnol **17:** 708–711

Hothorn M, Wolf S, Aloy P, Greiner S, Scheffzek K (2004) Structural insights into the target specificity of plant invertase and pectin methylesterase inhibitory proteins. Plant Cell **16:** 3437–3447

Huber SC, Huber JL (1996) Role and regulation of sucrose-phosphate synthase in higher plants. Annu Rev Plant Physiol Plant Mol Biol **47:** 431–444

Iglesias DJ, Tadeo FR, Legaz F, Primo-Millo E, Talon M (2001) In vivo sucrose stimulation of colour change in citrus fruit epicarps: interactions between nutritional and hormonal signals. Physiol Plant **112:** 244–250

Ito Y, Kitagawa M, Ihashi N, Yabe K, Kimbara J, Yasuda J, Ito H, Inakuma T, Hiroi S, Kasumi T (2008) DNA-binding specificity, transcriptional activation potential, and the rin mutation effect for the tomato fruit-ripening regulator RIN. Plant J **55:** 212–223

Jin Y, Ni DA, Ruan YL (2009) Posttranslational elevation of cell wall invertase activity by silencing its inhibitor in tomato delays leaf senescence and increases seed weight and fruit hexose level. Plant Cell **21:** 2072–2089

Kanayama Y, Dai N, Granot D, Petreikov M, Schaffer A, Bennett AB (1997) Divergent fructokinase genes are differentially expressed in tomato. Plant Physiol **113:** 1379–1384

Kandel-Kfir M, Damari-Weissler H, German MA, Gidoni D, Mett A, Belausov E, Petreikov M, Adir N, Granot D (2006) Two newly identified membrane-associated and plastidic tomato HXKs: characteristics, predicted structure and intracellular localization. Planta **224:** 1341–1352

Karimi M, Inzé D, Depicker A (2002) GATEWAY vectors for *Agrobacterium*-mediated plant transformation. Trends Plant Sci **7:** 193–195

Klann EM, Chetelat RT, Bennett AB (1993) Expression of acid invertase gene controls sugar composition in tomato (Lycopersicon) fruit. Plant Physiol **103:** 863–870

Klann EM, Hall B, Bennett AB (1996) Antisense acid invertase (TIV1) gene alters soluble sugar composition and size in transgenic tomato fruit. Plant Physiol **112:** 1321–1330

Klann E, Yelle S, Bennett AB (1992) Tomato fruit acid invertase complementary DNA: nucleotide and deduced amino acid sequences. Plant Physiol **99:** 351–353

Klee HJ, Giovannoni JJ (2011) Genetics and control of tomato fruit ripening and quality attributes. Annu Rev Genet **45:** 41–59

Kocal N, Sonnewald U, Sonnewald S (2008) Cell wall-bound invertase limits sucrose export and is involved in symptom development and inhibition of photosynthesis during compatible interaction between tomato and *Xanthomonas campestris* pv *vesicatoria*. Plant Physiol **148:** 1523–1536

Koch K (2004) Sucrose metabolism: regulatory mechanisms and pivotal roles in sugar sensing and plant development. Curr Opin Plant Biol **7:** 235–246

Li Z, Palmer WM, Martin AP, Wang R, Rainsford F, Jin Y, Patrick JW, Yang Y, Ruan YL (2012) High invertase activity in tomato reproductive organs correlates with enhanced sucrose import into, and heat tolerance of, young fruit. J Exp Bot **63:** 1155–1166

Link M, Rausch T, Greiner S (2004) In Arabidopsis thaliana, the invertase inhibitors AtC/VIF1 and 2 exhibit distinct target enzyme specificities and expression profiles. FEBS Lett **573:** 105–109

Long JC, Zhao W, Rashotte AM, Muday GK, Huber SC (2002) Gravity-stimulated changes in auxin and invertase gene expression in maize pulvinal cells. Plant Physiol **128:** 591–602

Lunn JE, MacRae E (2003) New complexities in the synthesis of sucrose. Curr Opin Plant Biol **6:** 208–214

Martel C, Vrebalov J, Tafelmeyer P, Giovannoni JJ (2011) The tomato MADS-box transcription factor RIPENING INHIBITOR interacts with promoters involved in numerous ripening processes in a COLORLESS NONRIPENING-dependent manner. Plant Physiol **157:** 1568–1579

Mason G, Provero P, Vaira AM, Accotto GP (2002) Estimating the number of integrations in transformed plants by quantitative real-time PCR. BMC Biotechnol **2:** 20

Menu T, Rothan C, Dai N, Petreikov M, Etienne C, Destrac-Irvine A, Schaffer A, Granot D, Ricard B (2001) Cloning and characterization of a cDNA encoding hexokinase from tomato. Plant Sci **160:** 209–218

Miron D, Schaffer AA (1991) Sucrose phosphate synthase, sucrose synthase, and invertase activities in developing fruit of Lycopersicon esculentum Mill. and the sucrose accumulating Lycopersicon hirsutum Humb. and Bonpl. Plant Physiol **95:** 623–627

Moore S, Payton P, Wright M, Tanksley S, Giovannoni J (2005) Utilization of tomato microarrays for comparative gene expression analysis in the Solanaceae. J Exp Bot **56:** 2885–2895

Murashige T, Skoog F (1962) A revised medium for rapid growth and bio assays with tobacco tissue cultures. Physiol Plant **15:** 473–497

Proels RK, Roitsch T (2009) Extracellular invertase LIN6 of tomato: a pivotal enzyme for integration of metabolic, hormonal, and stress signals is regulated by a diurnal rhythm. J Exp Bot **60:** 1555–1567

Qin G, Wang Y, Cao B, Wang W, Tian S (2012) Unraveling the regulatory network of the MADS box transcription factor RIN in fruit ripening. Plant J **70:** 243–255

Rausch T, Greiner S (2004) Plant protein inhibitors of invertases. Biochim Biophys Acta **1696:** 253–261

Rolland F, Moore B, Sheen J (2002) Sugar sensing and signaling in plants. Plant Cell (Suppl) **14:** S185–S205

Ruan YL, Jin Y, Yang YJ, Li GJ, Boyer JS (2010) Sugar input, metabolism, and signaling mediated by invertase: roles in development, yield potential, and response to drought and heat. Mol Plant **3:** 942–955

Saravanan RS, Rose JKC (2004) A critical evaluation of sample extraction techniques for enhanced proteomic analysis of recalcitrant plant tissues. Proteomics **4:** 2522–2532

Schmittgen TD, Livak KJ (2008) Analyzing real-time PCR data by the comparative C(T) method. Nat Protoc **3:** 1101–1108

Sturm A (1999) Invertases. Primary structures, functions, and roles in plant development and sucrose partitioning. Plant Physiol **121:** 1–8

Sumner JB (1921) Dinitrosalicylic acid: a reagent for the estimation of sugar in normal and diabetic urine. J Biol Chem **47:** 5–9

Télef N, Stammitti-Bert L, Mortain-Bertrand A, Maucourt M, Carde JP, Rolin D, Gallusci P (2006) Sucrose deficiency delays lycopene accumulation in tomato fruit pericarp discs. Plant Mol Biol **62:** 453–469

Vaughn MW, Harrington GN, Bush DR (2002) Sucrose-mediated transcriptional regulation of sucrose symporter activity in the phloem. Proc Natl Acad Sci USA **99:** 10876–10880

Vrebalov J, Ruezinsky D, Padmanabhan V, White R, Medrano D, Drake R, Schuch W, Giovannoni J (2002) A MADS-box gene necessary for fruit ripening at the tomato ripening-inhibitor (rin) locus. Science **296:** 343–346

Wang F, Smith AG, Brenner ML (1993) Isolation and sequencing of tomato fruit sucrose synthase cDNA. Plant Physiol **103:** 1463–1464

Wang Y, Wang W, Cai J, Zhang Y, Qin G, Tian S (2014) Tomato nuclear proteome reveals the involvement of specific E2 ubiquitin-conjugating enzymes in fruit ripening. Genome Biol **15:** 548

Wiśniewski JR, Zougman A, Nagaraj N, Mann M (2009) Universal sample preparation method for proteome analysis. Nat Methods **6:** 359–362

Yu X, Wang X, Zhang W, Qian T, Tang G, Guo Y, Zheng C (2008) Antisense suppression of an acid invertase gene (MAI1) in muskmelon alters plant growth and fruit development. J Exp Bot **59:** 2969–2977

Zhong S, Fei Z, Chen YR, Zheng Y, Huang M, Vrebalov J, McQuinn R, Gapper N, Liu B, Xiang J, et al (2013) Single-base resolution methylomes of tomato fruit development reveal epigenome modifications associated with ripening. Nat Biotechnol **31:** 154–159

Zhu Z, Liu R, Li B, Tian S (2013) Characterisation of genes encoding key enzymes involved in sugar metabolism of apple fruit in controlled atmosphere storage. Food Chem **141:** 3323–3328

Zhu Z, Zhang ZQ, Qin GZ, Tian SP (2010) Effects of brassinosteroids on postharvest disease and senescence of jujube fruit in storage. Postharvest Biol Technol **56:** 50–55